

Standard Model Top Quark Asymmetry at the Fermilab Tevatron

M. T. Bowen,^{1,*} S. D. Ellis,^{1,†} and D. Rainwater^{2,‡}

¹*Dept. of Physics, University of Washington, Seattle, WA 98195*

²*Dept. of Physics and Astronomy,
University of Rochester, Rochester, NY 14627*

(Dated: November 5, 2018)

Abstract

Top quark pair production at proton-antiproton colliders is known to exhibit a forward-backward asymmetry due to higher-order QCD effects. We explore how this asymmetry might be studied at the Fermilab Tevatron, including how the asymmetry depends on the kinematics of extra hard partons. We consider results for top quark pair events with one and two additional hard jets. We further note that a similar asymmetry, correlated with the presence of jets, arises in specific models for parton showers in Monte Carlo simulations. We conclude that the measurement of this asymmetry at the Tevatron will be challenging, but important both for our understanding of QCD and for our efforts to model it.

arXiv:hep-ph/0509267v2 9 Jan 2006

*Electronic address: mtb6@u.washington.edu

†Electronic address: ellis@phys.washington.edu

‡Electronic address: rain@pas.rochester.edu

I. INTRODUCTION

The matter content of the highly successful Standard Model (SM) of particle physics was generally considered to be fully revealed after the discovery of the top quark in 1994 [1]. While the exact mechanism of electroweak symmetry breaking (EWSB) remains undetermined [2], the unusually large top quark mass [3, 4], of the same size as the EWSB scale, suggests that the top quark may play a special role. Taking a closer experimental look at the top quark is therefore high on our list of priorities – not to mention that its quantum numbers (other than mass) and couplings to other SM particles are only crudely known, or not known at all [5]. Furthermore, the production and subsequent decay of the top quark at current and future collider experiments is a serious background to many new physics searches. Thus it is essential to study top quark production in much more detail, and eventually to be able to simulate it accurately in Monte Carlo background studies.

The top quark sample that exists today, exclusively from Runs I and II of the Fermilab Tevatron, is rather small, a few hundred events. This shall soon increase by an order of magnitude or more. The Tevatron experiments CDF and DØ are beginning to study the amount of additional jet activity in top quark pair events, and early indications are that it is non-trivial [6]. There are also hints in the data from Run I that the kinematic distribution of the top quark pairs' decay products exhibit a charge asymmetry [7].

We reexamine QCD top quark pair production in $p\bar{p}$ collisions at Tevatron Run II energy, with special attention to the asymmetries in the production process and to the correlation of the asymmetries with extra radiation in top quark pair events. In fact, the presence of both the asymmetries and extra radiation have been theoretically expected for some time, but neither the structure of the asymmetries nor their correlations with extra radiation are fully reproduced by the standard tools used in experimental analysis. We make the case here that it is now time to study the asymmetry and its correlation with the extra radiation in detail. In Sec. II we review inclusive QCD top quark pair production at hadron colliders, including known next-to-leading order (NLO) effects. Previous work had identified an overall asymmetry for top quark pairs at leading order (LO) [8] and NLO [9], although it did not identify all the kinematic features present. We present updated results for the asymmetry at NLO, for both inclusive and exclusive samples. In Sec. III we present new results for the real emission component of inclusive $t\bar{t}$ production, where the asymmetry is shown as a differential distribution as a function of the kinematics of the extra hard radiation. We provide an analysis of the likely statistical uncertainties in a variety of scenarios with various luminosities, kinematic cuts and tagging efficiencies. We do not consider the questions of systematics and background rates in any detail. In Sections IV and V we study the asymmetry for $t\bar{t}$ production in the zero jet exclusive sample (additional jet activity is vetoed) and double jet sample, respectively. Section VI provides a discussion of the level of asymmetry that can be found in parton-shower Monte Carlo (PSMC) results where the NLO perturbative (coherent) asymmetry effects, as described in the previous sections, are not present. Finally we review our results and conclude in Section VII.

II. INCLUSIVE QCD TOP QUARK PAIR PRODUCTION

At LO, $t\bar{t}$ production is totally charge-conjugation symmetric for both production mechanisms, quark- and gluon-fusion: $q\bar{q} \rightarrow t\bar{t}$ and $gg \rightarrow t\bar{t}$. As a consequence, the angular distributions of the t and \bar{t} are totally symmetric for $p\bar{p}$ collisions. However, at higher orders

in α_s , this no longer remains true for all subprocesses.

As was pointed out almost two decades ago [8], not all processes involving additional partons are symmetric under charge conjugation with respect to the incoming proton and anti-proton beams. The process $gg \rightarrow t\bar{t}g$ is, but the processes $q\bar{q} \rightarrow t\bar{t}g$ and $qg \rightarrow t\bar{t}q$ are not. Processes involving initial state valence quarks will therefore exhibit a forward-backward asymmetry. This is caused by interference between initial- and final-state gluon emission (or its crossed process), analogous to what happens in QED, *e.g.*, the forward-backward asymmetry in $e^+e^- \rightarrow \mu^+\mu^-\gamma$ or other heavy fermion pairs [10]. Because $t\bar{t}$ production at the Tevatron is dominated at the 90% level by $q\bar{q}$ annihilation, we can expect the $q\bar{q}$ subprocess' asymmetry to be closely reflected in the total sample.

When the $p\bar{p} \rightarrow t\bar{t}$ cross section was calculated more fully at NLO [11], an asymmetry due to virtual corrections was noticed. It arises from an interference between the color-singlet 4-point (box) virtual correction and the Born term for the process $q\bar{q} \rightarrow t\bar{t}$. Ref. [9] examined this asymmetry more closely, although still inclusively and integrated over the phase space of the additional parton. It was found that the virtual contribution produces an asymmetry opposite in sign to and larger than that of the real emission component. For the forward-backward inclusive asymmetry defined in terms of the top quark rapidity y_t ¹,

$$A_{FB}^t = \frac{N_t(y_t > 0) - N_t(y_t < 0)}{N_t(y_t > 0) + N_t(y_t < 0)}, \quad (1)$$

Ref. [9] calculated a value of 4 – 5% for the Tevatron Run I, $\sqrt{s} = 1.8$ TeV, and top quark mass $m_t = 175$ GeV.

A. Recalculation of top quark asymmetry

To provide a connection to the previous work outlined above, we have recalculated the top and anti-top quark distributions for Tevatron Run II, $\sqrt{s} = 1.96$ TeV, using the NLO Monte Carlo code MCFM [12] with the updated top quark mass, $m_t = 178$ GeV, and structure functions of CTEQ6 [13] (set L1 for LO, M for NLO). We show our results in Fig. 1 for the LO and NLO inclusive calculations, and also for the $t\bar{t}0j$ exclusive calculations. We define this last quantity as the NLO $t\bar{t}$ inclusive rate minus the LO $t\bar{t}j$ inclusive rate above some cutoff, $p_T(j) > p_T(j, min)$ and inside some rapidity region $|\eta(j)| < \eta(j, max)$. (Note that inclusive NLO $t\bar{t}$ and LO $t\bar{t}j$ are the same order in α_s .) Thus we have

$$\sigma_{t\bar{t}0j}^{\text{excl}} = \sigma_{t\bar{t}}^{\text{NLO}} - \sigma_{t\bar{t}j}^{\text{LO}} \left(p_T(j) > p_T(j, min), |\eta(j)| < \eta(j, max) \right). \quad (2)$$

The $t\bar{t}0j$ exclusive rate corresponds to the total $t\bar{t} + X$ rate with a jet veto applied above some p_T inside some fiducial region of rapidity in the detector. Here we use the cutoffs

$$p_T(j) > 20 \text{ GeV}, \quad |\eta(j)| < 3.0.$$

This fiducial region is based on the Run II capabilities of the CDF and DØ detectors. It is important to note that, in order to evaluate the perturbative $t\bar{t}j$ asymmetry described

¹ Here we use rapidity, y , instead of polar angle, θ , since rapidity is conventional for hadron collider experiments. For massless particles, rapidity y is equal to pseudorapidity η .

above, the calculation *must* employ the exact matrix elements. Since parton-shower Monte Carlo tools such as PYTHIA [14], HERWIG [15] and SHERPA [16] do not include the full interference effects in the parton radiation that produce the asymmetry, they cannot be used to predict the asymmetry. However, as we will discuss later, the soft radiation models used in the Monte Carlos are capable of producing certain kinds of asymmetries, which must be understood in order to accurately analyze any asymmetries that may be in the experimental data. In our perturbative calculations the minimum p_T kinematic cut protects us from the soft singularity present in the $t\bar{t}g$ final state. We verify that this is sufficient by checking that $\sigma_{t\bar{t}j} \ll \sigma_{t\bar{t}}$. For the kinematic cuts defined above, MCFM gives $\sigma_{t\bar{t}} = 5.9 pb$ and $\sigma_{t\bar{t}j} = 1.1 pb$. Their ratio is only 0.19, indicating that the calculation is perturbative. However, because $\sigma_{t\bar{t}j}$ is calculated only at LO, there is a considerable residual uncertainty of probably a factor of two at the Tevatron energy. This means there is also a larger uncertainty in the $t\bar{t}0j$ exclusive rate compared to the NLO inclusive rate, since the former is effectively calculated at LO. For example, we choose the top quark mass, m_t , as the factorization and renormalization scales in our benchmark cross section. This is conservative because it lies at the low end of our estimates for the LO $t\bar{t}j$ rate. However, if we choose scales that take into account the softness of the additional radiation parton, *e.g.*, $p_T(j)$, the cross section can be twice as large as our benchmark point. Even in this case we would still regard our result as perturbative. For a final analysis from Run II data, knowing the NLO $t\bar{t}j$ rate will probably become necessary. Fortunately, this calculation is underway [17].

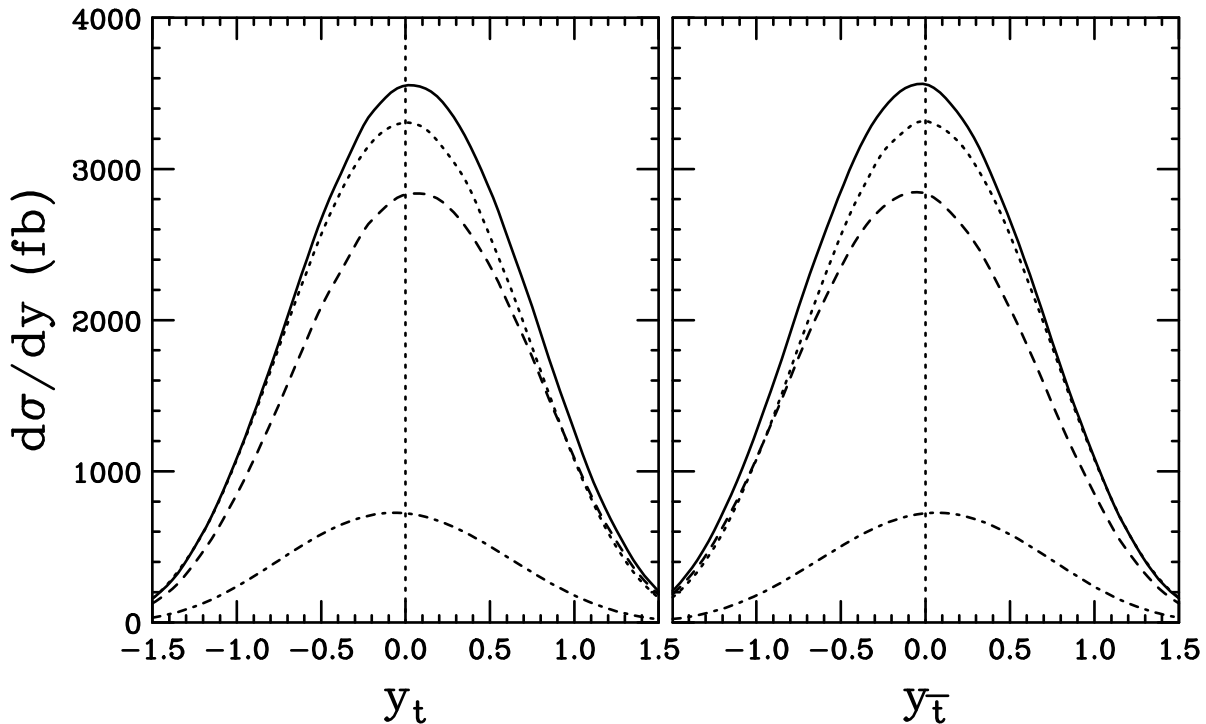


FIG. 1: Differential cross section distributions as a function of the top (left) and anti-top (right) quark rapidities, produced in $p\bar{p}$ collisions at the Tevatron in Run II, $\sqrt{s} = 1.96$ TeV. Shown are the LO $t\bar{t}$ inclusive (dotted), $t\bar{t}$ NLO inclusive (solid), LO $t\bar{t}j$ inclusive (dot-dashed) and $t\bar{t}0j$ exclusive (dashed) predictions. We define the LO $t\bar{t}j$ inclusive rate as that where the additional final-state parton has $p_T(j) > 20$ GeV and $|\eta(j)| < 3$. The $t\bar{t}0j$ exclusive rate is then the NLO inclusive rate minus the LO $t\bar{t}j$ inclusive rate.

The structure of the asymmetry described above can be seen in Fig. 1. First note that the LO $t\bar{t}$ inclusive cross section (dotted curve) is symmetric about $y = 0$ in both panels, *i.e.*, for both t and \bar{t} . Comparison of this symmetric curve with the (solid curve) NLO inclusive result indicates that the latter curve is (slightly) shifted to larger y for t (left panel) and smaller y for \bar{t} (right panel) corresponding to a positive asymmetry. The $t\bar{t}0j$ exclusive cross section (dashed curve) exhibits a shift that is similar in terms of magnitude and direction. On the other hand, the LO $t\bar{t}j$ inclusive cross section (dot-dashed curve) is shifted in the opposite direction in each panel yielding a negative asymmetry. Thus we conclude that the real emission corrections tend to push the top quark backward, opposite to the proton beam direction, while the virtual corrections push it forward, in the direction of the proton beam. The virtual corrections are larger as indicated by the qualitative agreement between the overall NLO inclusive distribution (solid curve) and the $t\bar{t}0j$ exclusive distribution (dashed curve). The y_t and $y_{\bar{t}}$ distributions are mirror images of each other, as required by CP -invariance of QCD.

process	A_{FB}^t
LO $t\bar{t}$ inclusive	0
NLO $t\bar{t}$ inclusive	3.8
LO $t\bar{t}j$ inclusive	-6.9
$t\bar{t}0j$ exclusive	6.4

TABLE I: Top quark forward-backward asymmetry in $p\bar{p} \rightarrow t\bar{t}$ production at Tevatron Run II, $\sqrt{s} = 1.96 \text{ TeV}$, for top quark mass $m_t = 178 \text{ GeV}$. The $1j$ inclusive and $t\bar{t}0j$ exclusive rates are defined by $p_T(j) > 20 \text{ GeV}$ and $|\eta(j)| < 3.0$. $A_{FB}^{\bar{t}} = -A_{FB}^t$ by CP -invariance. The cross sections were calculated with MCFM [12]).

Table I shows our numerical results for A_{FB}^t that arise from integrating over the distributions in Fig. 1. Note that, as expected, these estimates of the magnitude of the $t\bar{t}$ asymmetries depend on the choice of factorization and renormalization scales. For example, with both scales set to $m_t/2$, m_t , and $2m_t$, the NLO inclusive $t\bar{t}$ asymmetries are 5.5%, 3.8%, 2.8%, respectively. In this paper, we examine all asymmetries with both scales set to m_t . Since the strong interaction is separately C and P symmetric and the initial state in the $p\bar{p}$ process is a CP eigenstate, overall CP -invariance requires that $A_{FB}^{\bar{t}} = -A_{FB}^t$. At the same time, since the initial state is not an eigenstate of C (or P) alone, we can have $A_{FB}^{\bar{t}} \neq A_{FB}^t \neq 0$. As expected from the distributions, the LO asymmetry vanishes, the NLO inclusive and $t\bar{t}0j$ exclusive asymmetries are positive, and the asymmetry result for the $t\bar{t}j$ inclusive distribution is negative. When considering these results, it is important to recall that the magnitudes (but not the signs) of the last two entries in the table depend on the p_T cut defining the jets, which in this case has the value $p_T(j) > 20 \text{ GeV}$. NLO final states with extra real emission above the cut are included in the LO $t\bar{t}j$ inclusive sample and exhibit a negative asymmetry. The corresponding real emission configurations below the cut are included in the $t\bar{t}0j$ exclusive result, where they partially cancel the virtual contributions with a positive asymmetry reducing the net asymmetry in this term. Thus we can vary the magnitudes of the last two entries in the table up and down together by varying the jet-defining p_T cut (larger magnitudes for a smaller cut and vice versa). Our numerical results differ slightly from those of Ref. [9] due partly to the higher energy, but also due to the different PDF set used here.

The obvious question to ask is, can Tevatron Run II measure the various inclusive and exclusive asymmetries predicted by perturbative QCD? Observing the top quark asymmetry in a collider experiment such as Tevatron Run II is complicated by the difficulty in accurately reconstructing the underlying parton kinematics from the measurements of jets, compared to leptons. Because top quarks are produced at the Tevatron with transverse momentum typically smaller than their mass, their decay products are distributed over a large solid angle. Mismeasurement of individual jets thus results in a non-negligible uncertainty in the top quark direction. One should then look instead at the decay products, since any forward-backward top quark asymmetry will manifest itself in the daughter particles as well, albeit with possibly different magnitudes. The b jets are tagged, but their charge is extremely difficult to determine, so they are not good candidates. Nor are hadronically-decaying W bosons, again because of jet mismeasurement issues, but also because light-flavor jet charges cannot be determined at all. Instead we propose to use the asymmetry of the final state leptons (electron or muon) from W decays, since the the direction of leptons is extremely well-measured.

Top quark pairs decay to two possible final states containing a lepton: both top quarks can decay to $b\ell\nu$, where $\ell = e, \mu$, which we call the “dilepton” final state; or one decays to $b\ell\nu$ while the other decays to bjj , which we call the “lepton+jets” final state. The cleanest sample experimentally is the dilepton sample, although it occurs at only about 1/6 the rate of the lepton+jets channel. Assuming both b jets are tagged, the dilepton sample has practically no background from other SM processes, while the lepton+jets channel has a signal to background (S:B) ratio of about 6:1 [18]. The dilepton channel has the added advantage that there is no confusion between the additional radiated hard jet in the event and jets from the W boson decay, as in the lepton+jets sample. Since these events include jets along with the leptons, we will find it informative to examine the correlations between the lepton forward-backward asymmetry and the kinematic properties of the jets.

To obtain a handle on the expected lepton asymmetries we calculate using matrix elements for $p\bar{p} \rightarrow t\bar{t}$ production, including decay spin correlations and treating the intermediate W bosons off-shell, as generated by MADGRAPH [19]. We evaluate cross sections at $\sqrt{s} = 2.0$ TeV and use factorization and renormalization scale choices of $\mu_f = \mu_r = m_t$ (the small dependence on the total energy and the factorization/renormalization scales will not be an issue here). Before top quark decays, the cross section is 4.87 pb, compared to 6.7-8.0 pb for the NLO+(N)NLL $t\bar{t}$ rate [20]. We will normalize our results to the NLO rate for our inclusive results; using the average of the two NLO results, 7.4 pb, the effective K-factor is 1.52.

To calculate cross sections for observable final states at the parton level, we use our LO MADGRAPH code normalized to the NLO rate, then impose generic kinematic cuts on the outgoing particles suitable for both $D\emptyset$ and CDF:

$$\begin{aligned}
& \not{p}_T > 20 \text{ GeV} , \\
& p_T(b) > 15 \text{ GeV} , \quad |\eta(b)| < 2.0 , \quad \Delta R(b, b) > 0.4 , \\
& p_T(j) > 20 \text{ GeV} , \quad |\eta(j)| < 2.0 , \quad \Delta R(j, j; j, b) > 0.4 , \\
& p_T(\ell) > 20 \text{ GeV} , \quad |\eta(\ell)| < 1.1 , \quad \Delta R(\ell, \ell) > 0.2 , \quad \Delta R(\ell, j; \ell, b) > 0.4 .
\end{aligned} \tag{3}$$

The cuts are very conservative compared to the CDF and $D\emptyset$ expectations for the majority of Run II, but reflect the present level of understanding of the detectors and are used in current top quark analyses [21, 22]. For example, muons can easily be identified out to a pseudorapidity of 2.0, and non- b jets can be identified for $p_T(j) > 15$ GeV. For both

the dilepton and lepton+jets final states we discuss below, we consider the possibility of increasing the statistics by loosening the cuts accordingly. We do not attempt to simulate detector effects.

Regardless of the decay mode, we define the lepton asymmetry as

$$A_{FB}^\ell = \frac{N(\eta_\ell > 0) - N(\eta_\ell < 0)}{N(\eta_\ell > 0) + N(\eta_\ell < 0)}, \quad (4)$$

where the lepton may be ℓ^+ or ℓ^- , depending on which is visible (or both, in dilepton events, but $A_{FB}^{\ell^+}$ and $A_{FB}^{\ell^-}$ are calculated separately). Once a cross section with cuts is obtained, the NLO-normalized number of expected events for a given luminosity and set of detector ID efficiencies is distributed into forward and backward bins such that the asymmetry is the same 3.8% as that predicted at NLO by MCFM *for the top quarks*. It is important to point out, as we will see later explicitly in the $t\bar{t}j$ Section III, that kinematic cuts can alter the asymmetry for a given subsample. Hence our procedure is only an approximation. However, as no NLO $t\bar{t}$ program yet has the capability to decay the top quarks with spin correlations intact at NLO, our approximation is the best we can accomplish at the moment. Hopefully it will be superseded in the near future.

B. Dilepton final state

When both top quarks decay leptonically, the final state in the detector is $b\bar{b}\ell^+\ell^-\cancel{p}_T$, where $\ell = e, \mu$ and \cancel{p}_T is missing energy transverse to the beam axis, resulting from the neutrinos which escape undetected. We assume that both b jets are tagged, rendering the backgrounds negligible. This is thus the cleanest top quark pair sample in the data. The cross section with dilepton kinematic cuts and NLO K-factor applied is 113 fb.

We begin with a very conservative baseline assumption of 20% for the double b -tagging efficiency, which we label ϵ_{2b} . For 4 fb^{-1} and straightforwardly combining the statistics of $D\bar{O}$ and CDF (*i.e.*, a factor of 2), we estimate about 180 events in the dilepton sample with two b tags summed over $\ell = e, \mu$. The statistical uncertainty on an asymmetry is given in Ref. [23]:

$$\delta A_{FB}^\ell = \frac{2\sqrt{N_F^\ell N_B^\ell}}{\sqrt{(N_F^\ell + N_B^\ell)^3}} = \frac{1 - (A_{FB}^\ell)^2}{2} \sqrt{\frac{1}{N_F^\ell} + \frac{1}{N_B^\ell}} \quad (5)$$

where $N_F^\ell(N_B^\ell)$ is the number of observed events with the lepton ℓ forward (backward). Taking CP as a good symmetry we have $A_{FB}^{\ell^+} = -A_{FB}^{\ell^-}$ ($N_F^{\ell^+} = N_B^{\ell^-}$, $N_B^{\ell^+} = N_F^{\ell^-}$) and we can combine the statistics of the ℓ^+ and ℓ^- channels. For the dilepton sample this means that each event contributes twice. Combining the two charges also yields a factor $\sqrt{2}$ improvement in overall significance of the asymmetry determination over the single sign analysis. We summarize the dilepton channel results in Table II. We see that the initial numbers for the dilepton channel yield an uncertainty in the asymmetry measurement of $\delta A_{FB}^\ell/A_{FB}^\ell \sim 1.4$, providing only a 0.7σ effect with the summed sign data. We conclude that it will be challenging to use the dilepton channel due to poor statistics, at least with our conservative assumptions. However, there are many opportunities for increasing the sample size.

Here we explore various prospects for improving the sample size coming from multiple sources, of varying likelihood. The results are illustrated in Table II. First, the lepton

cuts can be loosened by observing leptons out to a pseudorapidity of 2.0 instead of 1.1, which is already possible for muons. This adds $\sim 65\%$ to the observed rate. Lowering the p_T cut of only one lepton to 10 GeV adds another 15%. Another few percent improvement will automatically come from events where one or both W bosons decay to a tau lepton, which then decays to an electron or muon. Imposing looser lepton cuts but ignoring the contribution from taus, we obtain a rate enhancement of about a factor of 1.9 so that the uncertainty decreases slightly, to $\delta A_{FB}^\ell/A_{FB}^\ell \sim 1.0$. The measurement becomes 1σ as indicated in the second line of Table II.

We also expect that the b -tag efficiency should be improved noticeably, both by adding kinematic track information in a neural net analysis to the vertex tag, and by beginning to include soft lepton tags, which is about 10% per b [21]. Together, these highly likely improvements to b -jet tagging would enlarge the sample by another factor of 1.9. Third, Run II could achieve its “stretch” goal of about 8 fb^{-1} , which would double the sample. Taken together (the most optimistic scenario), these improvements would result in a dilepton sample more about seven times what our conservative scenario predicts. In this case, the asymmetry in the dilepton channel is still challenging, yielding a 2.0σ measurement of the inclusive asymmetry as indicated in the fourth line of Table II.

It is fair to ask how feasible these improvements are. The expanded lepton pseudorapidity coverage is a safe bet, while the lowered- p_T cut is possible but not guaranteed (and also doesn’t result in much gain, compared to increased angular coverage). The b -jet tagging efficiency will definitely improve noticeably with the addition of soft lepton tags, while the prospects for improved silicon vertex tags are not yet fully understood. We cannot guess at the total integrated luminosity of Run II, but anticipate continued efforts at improvement.

Another natural possibility to consider is requiring only one b -tag, which with the assumed improved tagging efficiency would increase the sample by about a factor of 2.2. While this approach introduces some SM background, the background contribution will not be large. Ultimately this must be taken into account, although it is beyond the scope of this paper. Ignoring the small contribution from background, a single b -tag strategy would result in an uncertainty of $\delta A_{FB}^\ell/A_{FB}^\ell \sim 0.34$ and yield a 2.9σ measurement as indicated in the fifth line in Table II. We note that it may also be possible to usefully study a zero b -tag dilepton sample. Half this sample, containing an $e + \mu$ mixed-flavor pair, has extremely low backgrounds. The primary background for the other half, ee or $\mu\mu$ events, arises from the Drell-Yan process with an intermediate Z boson with a substantial ($\sim 20\%$) asymmetry. We expect this background can be controlled by cutting away the Z -pole region and demanding extra jets.

We also mention one other possible scheme for improving the measurement in the dilepton sample. Instead of an asymmetry based on a single lepton being forward versus background in the laboratory frame, consider one based on the longitudinal ordering of the 2 leptons,

$$\bar{A}_{FB}^\ell = \frac{N(\eta_{\ell^+} > \eta_{\ell^-}) - N(\eta_{\ell^+} < \eta_{\ell^-})}{N(\eta_{\ell^+} > \eta_{\ell^-}) + N(\eta_{\ell^+} < \eta_{\ell^-})}. \quad (6)$$

A preliminary look at the inclusive asymmetry using MCFM [12] suggests that \bar{A}_{FB}^ℓ may be 50% larger than A_{FB}^ℓ . While the dilepton sample is likely not as statistically significant as lepton+jets, this observable may become more relevant if systematic uncertainties prove to be the larger problem.

Sample	$\int \mathcal{L} dt$ [fb ⁻¹]	cuts	ϵ_{2b}	$N_F^{\ell^+} + N_B^{\ell^-}$	$N_B^{\ell^+} + N_F^{\ell^-}$	$\frac{\delta A_{FB}^\ell}{A_{FB}^\ell}$	signif.
dilepton	4	tight	0.20	188	174	1.4	0.7 σ
dilepton	4	loose	0.20	360	334	1.0	1.0 σ
dilepton	4	loose	0.38	685	635	0.72	1.4 σ
dilepton	8	loose	0.38	1370	1270	0.51	2.0 σ
dilepton	8	loose	0.62*	3074	2849	0.34	2.9 σ
lepton+jets	4	tight	0.20	570	528	0.79	1.3 σ
lepton+jets	4	loose	0.20	864	801	0.64	1.6 σ
lepton+jets	4	loose	0.38	1642	1522	0.47	2.1 σ
lepton+jets	8	loose	0.38	3285	3044	0.33	3.0 σ
combined	4	tight	0.20	757	702	0.69	1.5 σ
combined	4	loose	0.20	1225	1135	0.54	1.8 σ
combined	4	loose	0.38	2327	2157	0.39	2.5 σ
combined	8	loose	0.38	4654	4314	0.28	3.6 σ
combined	8	loose	0.38*	6359	5893	0.24	4.2 σ

TABLE II: Numbers of forward and backward lepton events, combining ℓ^+ and ℓ^- samples (rounded to the nearest integer) and expected statistical uncertainty on the measured lepton asymmetry, A_{FB}^ℓ , for inclusive $t\bar{t}$ production in $p\bar{p}$ collisions at Tevatron Run II, $\sqrt{s} = 2.0$ TeV, for top quark mass $m_t = 178$ GeV, summed over the two detectors. The lepton asymmetry in each case is assumed to be that of the top quarks themselves, +3.8%. The upper block contains the result for the dilepton sample, the middle block for the lepton+jets sample, and the lower block for the combined samples. The total NLO cross section is taken to be 7.4 pb, the average of the results of Refs. [20]. “Tight” cuts refers to those of Eq. 3, while “loose” refers to the increased acceptance scenario described in Secs. IIB, IIC. The * entries represent using a single b -tag strategy for the dilepton sample.

C. Lepton+jets final state

A different approach to increasing the sample size is to consider the lepton+jets channel, which is slightly more than a factor six larger in branching ratio than the dilepton channel. After cuts, the LO cross section times NLO K-factor is 686 fb, approximately maintaining the ratio of lepton+jets to dilepton rates. This channel does have a larger background than dileptons, mostly from W +jets, which is not fully understood either theoretically or from data. However, with double b -jet tagging, S:B is about 6:1 [18], so for our purposes we assume a double b -tagging strategy and ignore background contamination. Naturally, the inherent asymmetries of the same final state from W +jets, about 20% in the untagged sample, must eventually be included, using exact matrix elements also for the background.

Again conservatively assuming a double b -jet tagging efficiency of 20%, we predict about 1100 events in 4 fb⁻¹ summed over both experiments. Note that for this channel each event only contributes once (a single lepton) to the measurement of the asymmetry, for a net improvement over the dilepton case of about a factor of 3. As indicated in the middle block of Table II this provides for an initial measurement: $\delta A_{FB}^\ell/A_{FB}^\ell \sim 0.8$ and statistical significance of 1.3 σ . As above we consider the impact of increasing the lepton acceptance range to $\eta(\ell) < 2.0$, lowering the lepton $p_T(j)$ cut to 15 GeV, and allowing for non- b jets from W decay also down to $p_T > 15$ GeV. This would increase the cross section by about

50% as indicated in the middle block of Table II. Prospects for improving this sample’s size from other sources, such as improved b -tagging and greater integrated luminosity, are the same as in the dilepton sample. In the most optimistic scenario of 8 fb^{-1} per experiment, a double b -tagging efficiency of 38% and utilizing the looser cuts, we find that the uncertainty in the asymmetry would be about $1/3$, leading to a 3σ measurement as indicated in Table II. Combining this and the dilepton channels would increase the statistical significance to more than 4σ as indicated in the bottom section of Table II.

III. DIFFERENTIAL ASYMMETRY IN TOP QUARK PAIR +1 JET EVENTS

Next we consider correlations between the lepton asymmetry and a single extra jet in the event not arising from the top quark decays. As in the inclusive case, for all our calculations we use matrix elements for $p\bar{p} \rightarrow t\bar{t}j$ production ($j = q, \bar{q}, g$ summed over four light quark flavors), including decay spin correlations and treating the intermediate W bosons off-shell, as generated by MADGRAPH [19]. The extra parton does not come from either of the on-shell top quark decays, *i.e.*, we do not include radiative decays. We calculate cross sections at $\sqrt{s} = 2.0 \text{ TeV}$ requiring the additional hard jet to have $p_T > 20 \text{ GeV}$ and $|\eta| < 2.0$, and use factorization and renormalization scale choices of $\mu_f = \mu_r = m_t$, which yields a perturbatively well-behaved result: before top quark decays, the cross section is 1.03 pb , compared to $6.7\text{-}8.0 \text{ pb}$ (avg. 7.4 pb) for the NLO+(N)NLL $t\bar{t}$ rate [20].

As noted in the previous section, choosing a more “physical” scale which takes into account the softness of the additional parton, the cross section rises to 2.0 pb , still a reasonable, perturbative result. The uncertainty on the inclusive $t\bar{t}j$ rate awaits a full NLO calculation [17], but our conservative choice of $\mu = m_t$ gives the lowest cross section and may be regarded as a conservative baseline. We will consider the possibility of larger normalization (by a factor of 2) in our numerical results. Note that our predictions for the asymmetry will not depend on the normalization, as discussed in the next section.

A. Dilepton final state

We assume that both b jets are tagged, so it is trivial to identify the additional parton. The additional parton in the data, however, will not always arise from the $t\bar{t}j$ “production-radiation” process as we have defined it. Approximately 50% of the time, *i.e.*, at a rate approximately equal to what we calculate here, the extra jet will be due to radiative top quark decay [24]. In the dilepton sample, this occurs when one of the b quarks emits a hard gluon. This defines the “decay-radiation” contribution. (As argued in Ref. [24] this separation between production- and decay-radiation, while approximate, is numerically reliable.) We discuss later how the production and decay contributions might be separated. As the calculations here describe the appearance of extra radiation in the production mechanism, they will exhibit the asymmetry characteristic of the LO $t\bar{t}j$ inclusive sample.

We could again show the overall asymmetry, as in Sec. II, integrated over all kinematics of the additional jet, but this is just a single number, with magnitude about $4 - 5\%$, the same as the asymmetry of the top quarks themselves. We do note that when the top quarks decay, leptons can be thrown preferentially back into the hemisphere opposite to the top quark flight direction, due to the spin of the top quark. Thus, the lepton asymmetry will not necessarily be the same as the top quark asymmetry show in Sec. II before decays. In

any case, the more interesting result lies in the asymmetry as a function of the kinematics of the additional jet. We first show A_{FB}^ℓ as a function of the p_T of the extra jet in Fig. 2. The corresponding version of Eq. 4

$$A_{FB}^\ell(p_T(j)) = \frac{N(\eta_\ell > 0, p_T(j)) - N(\eta_\ell < 0, p_T(j))}{N(\eta_\ell > 0, p_T(j)) + N(\eta_\ell < 0, p_T(j))}, \quad (7)$$

where, for example, $N(\eta_\ell > 0, p_T(j))$ is the number of events with a forward lepton and an extra jet with transverse momentum $p_T(j)$. As indicated in Fig. 2 this distribution is essentially constant at the overall asymmetry value. Despite the lack of structure, this result is important because it shows that the asymmetry is not dependent on the extra parton p_T cutoff, so our results are independent of uncertainty due to the choice of the perturbative cutoff in p_T . CP still tells us that $A_{FB}^{\ell^+}(p_T(j)) = -A_{FB}^{\ell^-}(p_T(j))$ as shown in the figure. Note also that, as expected, $A_{FB}^{\ell^+} < 0$, just as for the LO $t\bar{t}j$ inclusive sample.

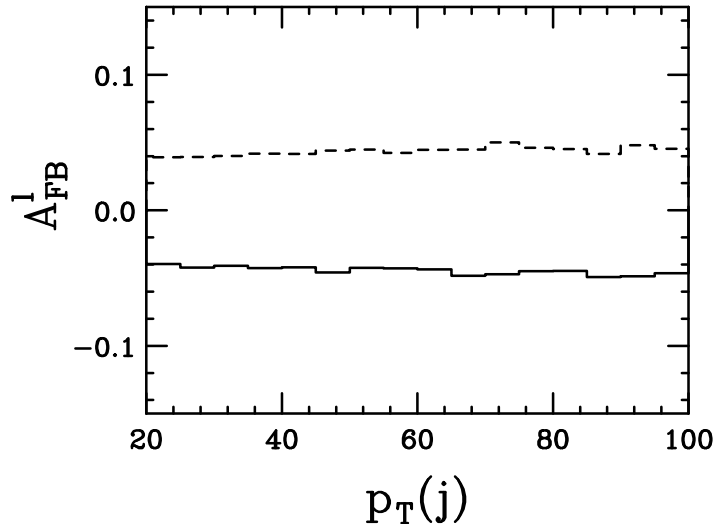


FIG. 2: Forward-backward lepton asymmetry in production-radiation $t\bar{t}j$ dilepton events as a function of the transverse momentum of the additional hard jet. The ℓ^+ (ℓ^-) distribution is the solid (dashed) curve. The two curves are CP -invariant up to the level of Monte Carlo statistical uncertainty.

The asymmetry with respect to the angular distribution of the additional jet is far more revealing. The distribution of interest is now

$$A_{FB}^\ell(\eta(j)) = \frac{N(\eta_\ell > 0, \eta(j)) - N(\eta_\ell < 0, \eta(j))}{N(\eta_\ell > 0, \eta(j)) + N(\eta_\ell < 0, \eta(j))}, \quad (8)$$

where CP invariance specifies that $A_{FB}^{\ell^+}(\eta(j)) = -A_{FB}^{\ell^-}(-\eta(j))$, *i.e.*, $A_{FB}^{\ell^+}$ and $A_{FB}^{\ell^-}$ are mirror images of each other about $\eta(j) = 0$. We show this asymmetry distribution in Fig. 3, separately for the different parton subprocess and for the combined result. Note that for each pair of distributions (for the 2 lepton charges) the CP relation just noted is satisfied, but not always in the same way. For the subprocess $gg \rightarrow t\bar{t}g$ the initial state is symmetric with respect to C alone requiring that $A_{FB}^{\ell^+}(\eta(j), gg) = A_{FB}^{\ell^-}(\eta(j), gg)$, so that CP now requires that the distributions are separately odd in the jet rapidity,

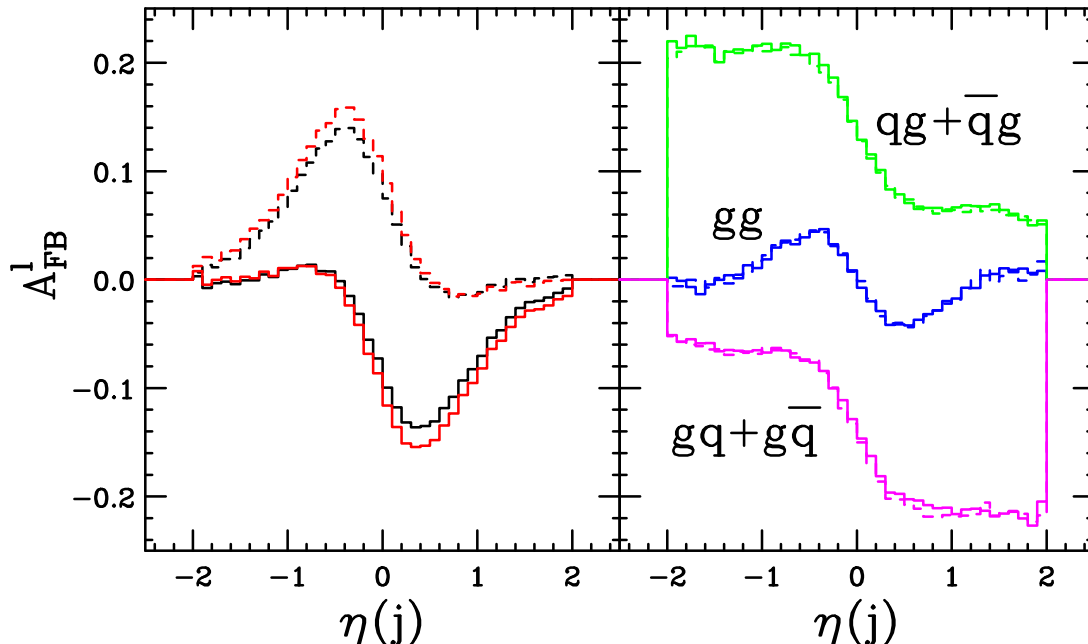


FIG. 3: Forward-backward lepton asymmetries for each subprocess in production-radiation $t\bar{t}j$ dilepton events as a function of the pseudorapidity of the additional hard jet. The ℓ^+ (ℓ^-) distributions are shown by the solid (dashed) curves. The left panel shows the dominant $q\bar{q}$ contribution to the asymmetry (the curves with the slightly larger magnitude for both ℓ^+ and ℓ^-) and the asymmetry for both charges for the total rate (the curves with the smaller magnitude). The small difference between $q\bar{q}$ and total arises from the contributions of the other parton channels, whose asymmetries are indicated in the right panel. Note the absence of any charge dependence in the curves in the right panel.

$A_{FB}^{\ell}(\eta(j), gg) = -A_{FB}^{\ell}(-\eta(j), gg)$. These constraints are in agreement with the corresponding (middle) curves in the right panel of Fig. 3. The specific form of these distributions suggests that for this subprocess the $t\bar{t}$ pair tends to recoil from the extra jet, *i.e.*, the t and \bar{t} quarks (and the leptons from their decays) tend to be in the same hemisphere while the recoiling jet is in the opposite hemisphere (a backward jet yields a positive asymmetry and conversely). Formally, the subprocesses containing a single quark line exhibit an inclusive asymmetry, as found in Ref. [9], although it is numerically extremely small. For the discussion here we note that the combinations $qg + \bar{q}g$ or $gq + g\bar{q}$, as in the upper and lower curves in the right panel of Fig. 3, are strictly not C symmetric states due to the differences between q and \bar{q} distributions within a proton (or antiproton). Thus it does *not* follow that $A_{FB}^{\ell+}(\eta(j), qg + \bar{q}g) = A_{FB}^{\ell-}(\eta(j), qg + \bar{q}g)$, $A_{FB}^{\ell+}(\eta(j), gq + g\bar{q}) = A_{FB}^{\ell-}(\eta(j), gq + g\bar{q})$, even though these relations are approximately numerically true in our results in Fig. 3. So in this case the (exact) constraint of CP leads only to the approximate relation $A_{FB}^{\ell}(\eta(j), qg + \bar{q}g) \simeq -A_{FB}^{\ell}(-\eta(j), gq + g\bar{q})$. These features are illustrated in Fig. 3, where the boost effects from the vastly different average Feynman x values for quarks and gluons in the proton (antiproton) result in the specific shapes of the curves. Qualitatively the $qg + \bar{q}g$ subprocess tends to produce a $t\bar{t}$ pair in the forward hemisphere ($A_{FB}^{\ell} > 0$) with the extra jet recoiling into the backward hemisphere. Forward/backward are reversed for the $gq + g\bar{q}$ subprocess. Note that, after summing the qg, gq

and gq subprocesses, their net asymmetry integrates to approximately zero (over a symmetric interval in $\eta(j)$). Finally consider the $q\bar{q}$ subprocess, which not only dominates the total rate at Tevatron energies, but also exhibits the most interesting structure. The $q\bar{q}$ initial state is not separately invariant under C and P so that we have $A_{FB}^{\ell^+}(\eta(j), q\bar{q}) \neq A_{FB}^{\ell^-}(\eta(j), q\bar{q})$, while CP still guarantees that $A_{FB}^{\ell^+}(\eta(j), q\bar{q}) = -A_{FB}^{\ell^-}(-\eta(j), q\bar{q})$. The corresponding asymmetry distributions are illustrated in the left panel of Fig. 3 for both the $q\bar{q}$ subprocess (the curves with large magnitudes) and the total of all subprocesses (the curves with slightly smaller magnitudes). Note that for these distributions the asymmetry for a single lepton charge clearly does not integrate to zero. Qualitatively the $q\bar{q}$ subprocess tends to produce a t quark in the backward hemisphere and a \bar{t} antiquark at rest in the lab when the extra jet is forward, while a backward jet tends to correlate with a \bar{t} antiquark in the forward hemisphere and a t quark at rest in the lab.

As indicated in Fig. 3 the asymmetry reaches a maximum absolute value of around 14% for extra jet rapidity in the region around $|\eta(j)| \sim 0.4$, and, even averaged over the region $0 < \eta(j) < 1$ (for ℓ^+), the asymmetry is over 10%. The question of whether this can actually be measured is more difficult to answer. The dilepton production-radiation $t\bar{t}j$ cross section at LO with the “tight” cuts of Eq. 3 is 15.1 fb. With 4 fb^{-1} and a conservative double b -tag rate of 20%, Run II will then observe about 24 dilepton production-radiation $t\bar{t}j$ double- b -tagged events for DØ and CDF combined, based on the LO rate (and an approximately equal number of radiative $t\bar{t}j$ events). This is not enough statistics to perform even an overall asymmetry measurement, much less in a restricted region of $\eta(j)$. However, with the prospects for improving the sample size as discussed in Sec. II B, as well as the uncertainty in cross section normalization, this channel could possibly collect $\mathcal{O}(100)$ events and would then become interesting.

We present Fig. 4, the normalized angular-differential cross section overlaid on the (positive) lepton asymmetry, as a guide to how binning in $\eta(j)$ might be done depending on the ultimate statistics achieved in the dilepton channel. Fairly central jet rapidity features the largest asymmetry as well as large portion of the total rate. At a minimum, one

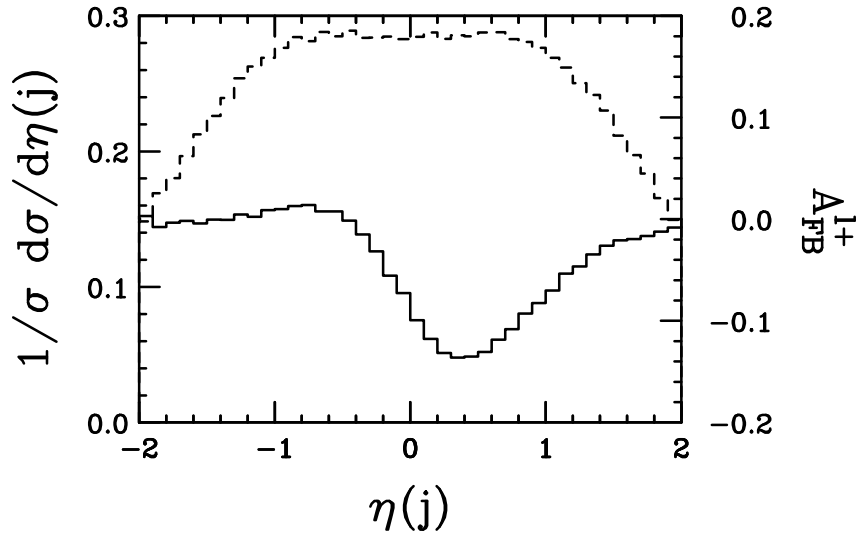


FIG. 4: Normalized differential cross section with respect to the extra jet pseudorapidity (dashed), overlaid with the total forward-backward positive lepton asymmetry (solid), in dilepton production-radiation $t\bar{t}j$ events with loose cuts as described in the text.

could use two bins, jet-forward and jet-backward, discarding the region beyond $|\eta_j| \sim 1$.

We have avoided the issue of the approximately equal-sized sample of radiative decay $t\bar{t}j$ dilepton events. This is obviously a non-trivial complication. Since the statistics of the dilepton channel are weak to begin with, we don't attempt to address it further here, except to note that radiative decay events are highly suppressed by imposing an angular cut $\Delta R_{jb} \gg 0.4$. For example, the cut $\Delta R_{jb} > 1.0$ reduces the radiative decay cross section by more than a factor two [24], but our calculations show only a 20% loss of production $t\bar{t}j$ dilepton events. In the lucky circumstance that Run II collects a very large dilepton top quark sample, this issue should be thoroughly investigated.

B. Lepton+jets final state

We again also consider the lepton+jets channel, which is slightly more than a factor six larger in branching ratio than the dilepton channel, although it does suffer from a slight background as discussed in Sec. II C. After cuts, the LO cross section is 88.9 fb, slightly less than a factor six larger than the dilepton channel with cuts.

The lepton+jets channel has one complication, that of correctly identifying which of the three non- b -tagged jets is the “extra” one, *i.e.*, the one that is not a top quark decay product. This situation is aggravated by the combinatorics, but can be largely addressed by imposing

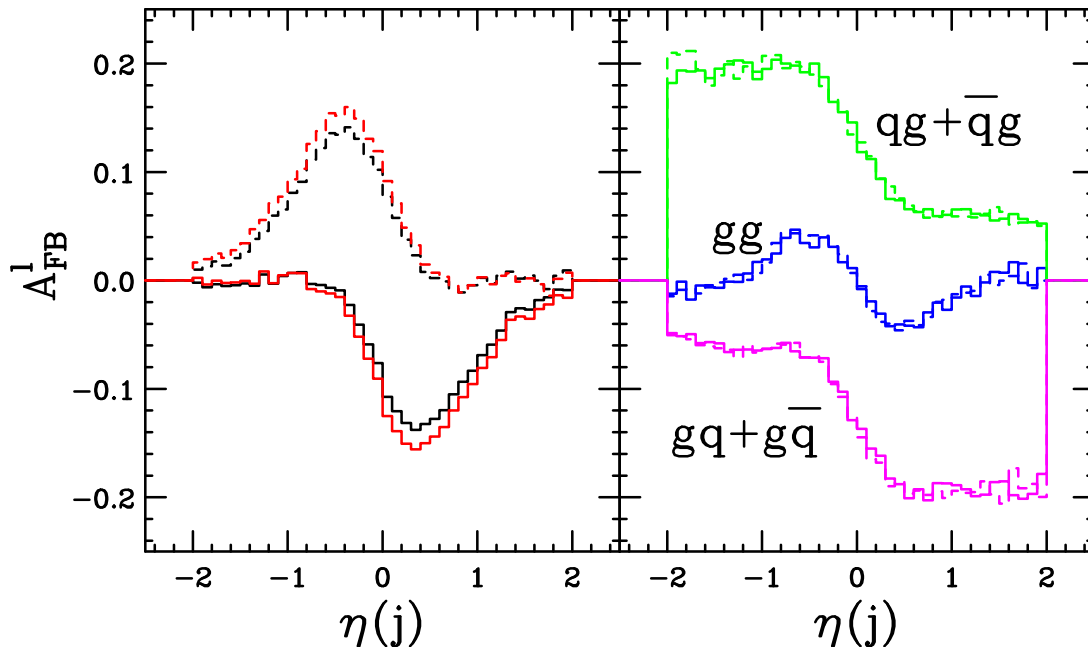


FIG. 5: Forward-backward lepton asymmetries for each subprocess in production-radiation $t\bar{t}j$ lepton+jets events as a function of the pseudorapidity of the additional hard jet. The ℓ^+ (ℓ^-) distributions are shown by the solid (dashed) curves. The left panel shows the dominant $q\bar{q}$ contribution to the asymmetry (the curves with the slightly larger magnitude for both ℓ^+ and ℓ^-) and the asymmetry for both charges for the total rate (the curves with the smaller magnitude). The small difference between $q\bar{q}$ and total arises from the contributions of the other parton channels, whose asymmetries are indicated in the right panel. Note the absence of any charge dependence in the curves in the right panel.

the W mass constraint on one jet pair, the top quark mass constraint on that pair and a b jet, and the transverse top mass constraint on the other b jet, the lepton and the missing transverse energy. We do not examine this issue further here, but expect misidentification effects due to kinematical combinatorics to be a minor correction. This issue should of course be examined in detail when the channel is studied with full detector simulation. Such mass constraints also remove the vast bulk of top quark decay-radiation events from the sample, as our minimum $p_T(j)$ requirement means that sample contamination from radiative events enters mostly via jet mismeasurement at the edges of invariant mass windows.

Fig. 5 shows the lepton asymmetry in production-radiation $t\bar{t}j$ lepton+jets events, similar to Fig. 3 for the dilepton case, also with the cuts of Eq. 3. This plot assumes that the additional jet, which did not come from a top decay, is determined with 100% accuracy, as discussed above. The asymmetry features in this sample are almost identical to those in the dilepton sample. The asymmetry as a function of extra jet p_T is flat as in the dilepton channel, and we do not show the corresponding figure here.

Again starting from the assumption of 20% efficiency for double b -jet tagging (no improvement over the current level), our LO estimate predicts about 142 events in 4 fb^{-1} for both experiments. Measuring the differential asymmetry therefore appears possible only for large pseudorapidity bins. Applying the loose cuts as in the inclusive sample gives about a factor 1.5 increase. Note that we keep the requirement that the extra jet has $p_T > 20 \text{ GeV}$, simply to keep our calculation confidently in the perturbative regime. Prospects for improving this sample's size from other sources, such as improved b -tagging, greater integrated luminosity, or cross section normalization, are the same as in the dilepton sample.

C. Numerical results

Here we make some simple estimates of the uncertainty that might be achieved on an A_{FB}^ℓ measurement in the inclusive $t\bar{t}j$ sample. The ideal objective in this case would be to map out the asymmetry with respect to the angular structure of the additional hard parton,

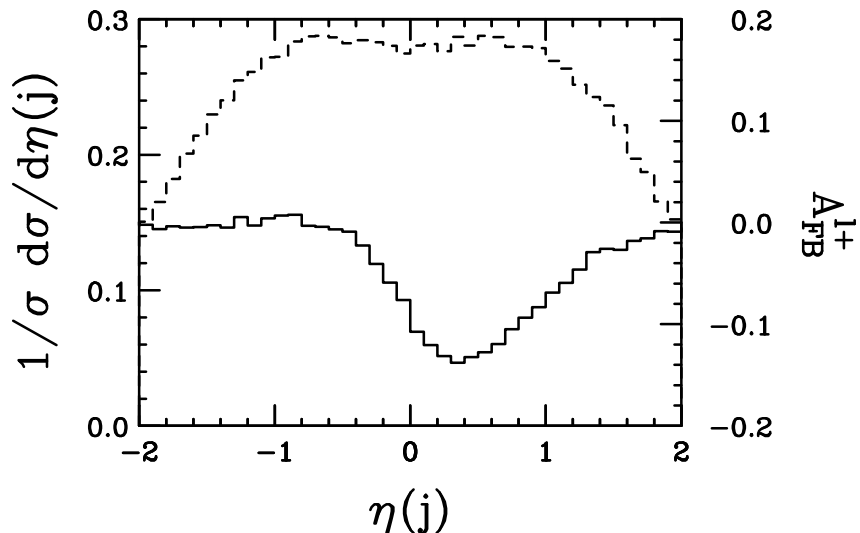


FIG. 6: Normalized differential $t\bar{t}j$ cross section with respect to the extra jet pseudorapidity (dashed), overlaid with the total forward-backward positive lepton asymmetry (solid), in lepton+jets events with loose cuts as described in the text.

which is additional information that the inclusive and exclusive $t\bar{t}$ samples do not have. We consider both the dilepton and lepton+jets samples, although the latter has far better statistics and is expected to largely avoid the complications of radiative top quark decay. We consider only the statistical uncertainty, as the most important systematic uncertainties are related to detector effects, which we cannot include; or the very small backgrounds in double b -tagged events, which are expected to be a much smaller uncertainty than the limited statistics will allow for.

Due to the limited statistics available, we select a single bin in extra jet pseudorapidity of $-0.1 < \eta(j) < 1.1$ ($-1.1 < \eta(j) < 0.1$) for ℓ^+ (ℓ^-). Varying this over a range of a few tenths either direction at either limit does very little to the overall uncertainty, while increasing the range to increase statistics results in an overall lower asymmetry, and vice versa, as seen in Fig. 6. The asymmetry in this bin is 11%.

We show our numerical results in Table III, which has a general format similar to Table II. As suggested by Figs. 4 and 6 approximately 1/3 of the events fall into the rapidity window noted above, $-0.1 < \eta(j) < 1.1$ ($-1.1 < \eta(j) < 0.1$) for $\ell^+(\ell^-)$. Thus, since the dilepton events still contribute twice, the 24 dilepton events mentioned above yield 16 counted leptons in the first line of the dilepton block ($24 \times 1/3 \times 2$) in Table III. For the lepton+jets sample the number of leptons is just 1/3 of the number of events so that 142 events become 47 leptons.

Sample	$\int \mathcal{L} dt$ [fb $^{-1}$]	cuts	ϵ_{2b}	A_{FB}^{ℓ}	$N_F^{\ell^+} + N_B^{\ell^-}$	$N_B^{\ell^+} + N_F^{\ell^-}$	$K_{NLO}^{t\bar{t}j}$	$\frac{\delta A_{FB}^{\ell}}{A_{FB}^{\ell}}$	signif.
dilepton	4	tight	0.20	-0.11	7	9	1	2.3	0.4 σ
dilepton	4	loose	0.20	-0.12	14	17	1	1.5	0.7 σ
dilepton	4	loose	0.38	-0.12	26	33	1	1.1	0.9 σ
dilepton	8	loose	0.38	-0.12	51	66	1	0.75	1.3 σ
dilepton	8	loose	0.38	-0.12	103	132	2	0.53	1.9 σ
lepton+jets	4	tight	0.20	-0.11	21	26	1	0.8	0.8 σ
lepton+jets	4	loose	0.20	-0.12	31	40	1	1.0	1.0 σ
lepton+jets	4	loose	0.38	-0.12	60	76	1	0.69	1.4 σ
lepton+jets	8	loose	0.38	-0.12	119	153	1	0.49	2.0 σ
lepton+jets	8	loose	0.38	-0.12	239	306	2	0.35	2.9 σ
combined	4	tight	0.20	-0.11	28	36	1	1.1	0.9 σ
combined	4	loose	0.20	-0.12	45	58	1	0.8	1.3 σ
combined	4	loose	0.38	-0.12	85	109	1	0.58	1.7 σ
combined	8	loose	0.38	-0.12	171	219	1	0.41	2.4 σ
combined	8	loose	0.38	-0.12	342	437	2	0.29	3.4 σ

TABLE III: Numbers of forward and backward lepton events combining ℓ^+ and ℓ^- samples (rounded to the nearest integer), and expected statistical uncertainty on the absolute value of the measured lepton asymmetry, A_{FB}^{ℓ} , for production-radiation $t\bar{t}j$ events in $p\bar{p}$ collisions at Tevatron Run II, $\sqrt{s} = 2.0$ TeV, for top quark mass $m_t = 178$ GeV, summed over the two detectors with $-0.1 < \eta(j) < 1.1$ for the extra jet. $K_{NLO}^{t\bar{t}j} = \frac{\sigma_{NLO}}{\sigma_{LO}}$ for the $t\bar{t}j$ rate. The upper block contains results for the dilepton sample, the middle block for lepton+jets sample, and the lower block for the combined samples. ‘‘Tight’’ cuts refers to those of Eq. 3, while ‘‘loose’’ refers to the possible increased acceptance as described in Sec. IIA. The first four lines in each block represent improvements in detector and machine performance, while the last line represents uncertainty in the $t\bar{t}j$ rate as discussed in Sec. III.

We have also included a column for the value of the asymmetry, $A_{FB}^{\ell^+}$, which is calculated directly from the cross sections and not the rounded numbers of leptons in the Table, and a column for the assumed K factor. For our very conservative baseline scenario with $\sigma_{NLO}/\sigma_{LO} = K = 1$, the measurement is effectively consistent with zero. The very likely scenario of increased lepton acceptance and expected b -tagging improvement, line 3, allows for a more interesting measurement. However, either increased luminosity or a fortuitous larger cross section, illustrated here with $\sigma_{NLO}/\sigma_{LO} = 2$ corresponding to a smaller choice of factorization/renormalization scale, would be required to allow the statistical significance of the measurement to reach the level of $3 - 4 \sigma$.

IV. ASYMMETRY IN TOP QUARK PAIR + 0 JET EXCLUSIVE EVENTS

We have seen that measuring the asymmetry in the inclusive $t\bar{t}$ sample may be doable but challenging, and that in the $t\bar{t}j$ inclusive production-radiation sample it will be extremely difficult. The inclusive $t\bar{t}$ sample suffers from a smaller asymmetry, while for the inclusive $t\bar{t}j$ sample statistics will be a larger problem. As seen in Sec. II, events without an additional hard jet should have a similar asymmetry to $t\bar{t}j$ events, although of opposite sign. Yet this sample would be approximately 6 times the size of the inclusive $t\bar{t}j$ sample, before any cuts are put on the jet rapidity. An obvious strategy is to experimentally attempt a jet veto on the $t\bar{t}$ inclusive sample to obtain an exclusive $t\bar{t}0j$ sample with better statistics than the inclusive $t\bar{t}j$ sample.

While definitely worth pursuing, this will not be straightforward. Recall that approximately as many events in inclusive $t\bar{t}$ production will have an additional hard jet from radiative top quark decay as from production radiation. One does not want to veto events with these jets. Certainly some fraction of the time DØ and CDF will be able to tell that the extra jet likely comes from radiative decay, based on the invariant mass of two or three jets reconstructing to a W boson, or for a b jet and the extra jet plus either two jets or a lepton to have an invariant mass (or transverse mass) equal to m_t . Determining how efficiently this can be done is beyond the scope of this paper, so we will ignore the complication of radiative top quark decays. Our goal in making estimates of how well one might measure A_{FB}^{ℓ} in the exclusive sample is simply to highlight the beneficial features of the larger asymmetry and the greater statistics.

Our procedure is to take the numbers of events expected in the inclusive $t\bar{t}$ sample based on the fraction of events that pass the cuts, as in Sec. II, and subtract from those forward and backward event numbers those from the $t\bar{t}j$ sample. The obvious deficiency in this is that the inclusive asymmetry is known only from a NLO calculation (necessarily) which does not include decays, so the asymmetry shift from kinematical cuts effects cannot yet be taken into account. Thus, one should not put too much faith in the exact values predicted, as we expect future calculations to shift them noticeably. Our calculations, however, do represent the state of the art at this time.

We show our numerical results in Table IV where the number of contributing events is approximately 18 times larger than in Table III due to the larger cross section ($\times 6$) and the absence of a jet rapidity cut ($\times 3$). As before, we consider tight and loose levels of kinematic cuts, low and high Tevatron integrated luminosity, pessimistic and optimistic b -tagging efficiencies, and a possible 1- b -tag strategy for the dilepton sample only. Note that if the $t\bar{t}j$ normalization is at the upper end of our cross section estimate, a factor of two larger than the conservative scale choice for the calculation, then the statistical significance of the

Sample	$\int \mathcal{L} dt$ [fb $^{-1}$]	cuts	ϵ_{2b}	A_{FB}^ℓ	$N_F^{\ell^+} + N_B^{\ell^-}$	$N_B^{\ell^+} + N_F^{\ell^-}$	$K_{NLO}^{t\bar{t}j}$	$\frac{\delta A_{FB}^\ell}{A_{FB}^\ell}$	signif.
dilepton	4	tight	0.20	0.044	176	161	1	1.4	0.7 σ
dilepton	4	loose	0.20	0.045	339	310	1	1.0	1.0 σ
dilepton	4	loose	0.38	0.045	644	589	1	0.75	1.3 σ
dilepton	8	loose	0.38	0.045	1288	1178	1	0.53	1.9 σ
dilepton	8	loose	0.62*	0.048	2891	2644	1	0.35	2.8 σ
dilepton	8	loose	0.38	0.052	1207	1087	2	0.53	1.9 σ
lepton+jets	4	tight	0.20	0.050	502	454	1	0.85	1.2 σ
lepton+jets	4	loose	0.20	0.052	764	689	1	0.69	1.4 σ
lepton+jets	4	loose	0.38	0.052	1452	1308	1	0.50	2.0 σ
lepton+jets	8	loose	0.38	0.052	2903	2616	1	0.35	2.8 σ
lepton+jets	8	loose	0.38	0.071	2521	2188	2	0.38	2.6 σ
combined	4	tight	0.20	0.049	678	615	1	0.73	1.4 σ
combined	4	loose	0.20	0.050	1103	999	1	0.57	1.7 σ
combined	4	loose	0.38	0.050	2096	1897	1	0.42	2.4 σ
combined	8	loose	0.38	0.050	4191	3794	1	0.29	3.4 σ
combined	8	loose	0.38*	0.048	5794	5260	1	0.25	4.0 σ
combined	8	loose	0.38	0.065	3728	3275	2	0.32	3.2 σ

TABLE IV: Numbers of forward and backward lepton events combining ℓ^+ and ℓ^- samples (rounded to the nearest integer), and expected statistical uncertainty on the absolute value of the measured lepton asymmetry, A_{FB}^ℓ , for production-radiation-vetoed $t\bar{t}0j$ exclusive events in $p\bar{p}$ collisions at Tevatron Run II, $\sqrt{s} = 2.0$ TeV, for top quark mass $m_t = 178$ GeV, summed over the two detectors. $K_{NLO}^{t\bar{t}j} = \frac{\sigma_{NLO}}{\sigma_{LO}}$ for the $t\bar{t}j$ rate. The upper block contains results for the dilepton sample, the middle block for the lepton+jets sample, and the lower block for the combined samples. ‘‘Tight’’ cuts refers to those of Eq. 3, while ‘‘loose’’ refers to the possible increased acceptance as described in Sec. II A. The first four lines in each block represent improvements in detector and machine performance, while the last two line represents uncertainty in the $t\bar{t}j$ rate as discussed in Sec. III. The fifth line in the first and last blocks (the * entries) represent using a single b -tag strategy for the dilepton sample as discussed in Sec. II B.

exclusive $t\bar{t}0j$ sample goes *down* slightly, due to the decreased sample size, which is partially compensated by the larger remaining asymmetry. As expected, the asymmetry in this sample is positive and somewhat larger in magnitude than the fully inclusive expectation of 3.8%. While the statistics are better than indicated in Table III, these results still suggest that with the standard luminosity, the conservative cross section and loose cuts, only a 2.4 σ measurement is possible. An integrated luminosity greater than 4 fb $^{-1}$ will be required for a more accurate determination of the asymmetry.

V. DIFFERENTIAL ASYMMETRY IN TOP QUARK PAIR + 2 JET EVENTS

The LO cross section for $t\bar{t}jj$ production at Tevatron Run II varies from 160 to 300 fb over the range of scale choices discussed earlier. We again calculate this with exact matrix elements from MADGRAPH, choosing $p_T(j) > 20$ GeV and $|\eta(j)| < 2.0$ as the limits in phase space integration for the extra jets. We further require $\Delta R_{jj} > 0.5$ for the extra jet pair

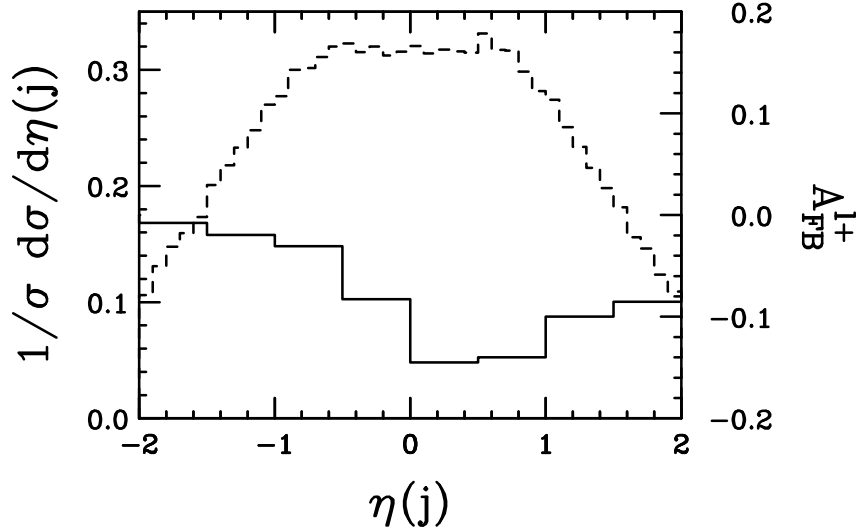


FIG. 7: Normalized differential $t\bar{t}j$ cross section with respect to the higher- p_T extra jet pseudo-rapidity (dashed), overlaid with the total forward-backward positive lepton asymmetry (solid), in lepton+jets events with loose cuts as described in the text.

to be separated from each other, to avoid the collinear singularity from gluon splitting. Compared to the 1–2 pb cross section for $t\bar{t}j$ production, this is approximately a factor 5 lower in statistics. Because of this, here we consider only the lepton+jets channel with the looser cuts and the improved b-tagging scenario.

Similar to the plot in Sec. III B we show the normalized differential cross section with respect to the rapidity of the higher- p_T of the two extra jets, as well as the differential asymmetry, in Fig. 7. The asymmetry shows similar structure to that of Fig. 6, although here we use larger binning as it takes considerably more computing time to obtain the same level of statistics for smaller bins. The optimal region to use to obtain the best statistical significance for an asymmetry measurement is about $-0.5 < |\eta(j)| < 2.0$, which includes approximately 2/3 of the total rate. For 8 fb^{-1} per experiment and two combined experiments, with conservative cross section normalization and a double b-tagging efficiency of 38% Run II (summing the 2 detectors) could expect about 76 events with average asymmetry $A_{FB}^{\ell^+} = -0.11$ over this region. This would yield only about a 1.0σ measurement. If the cross section is really a factor of two larger ($K = 2$), this would still only be about a 1.4σ measurement: interesting and worth pursuing, but difficult to achieve a useful level of precision.

VI. COMPARISON WITH PARTON SHOWER MONTE CARLO

Since Parton-shower Monte Carlo simulation packages, such as PYTHIA [14], HERWIG [15] and SHERPA [16], use only LO matrix elements, which do not exhibit the interference structure of the NLO matrix elements, they are not expected to reproduce the *inclusive* asymmetry seen at NLO. There is, however, the possibility that certain choices of the parameters that control the simulation of “color-coherence” in the showering/hadronization components of the Monte Carlo can lead to correlations that mimic the $t\bar{t}j$ and $t\bar{t}0j$ asymmetries observed in the NLO perturbative results. Recall that, while the individual partons describing the short distance scattering carry color charges, the long distance initial- and final-state

hadrons are all color neutral. The requirement of reassembling at long distances into color-neutral states requires correlations between the partons. Complete fixed-order perturbative calculations account explicitly for the color-coherence, at fixed order, but Monte Carlo simulations include color-flow correlations only approximately, based on various models. To illustrate this, we have studied $t\bar{t}$ dilepton production using PYTHIA [14].

We imposed the cuts of Eq. 3 on the b partons, leptons, and missing transverse momentum in Pythia-generated $t\bar{t}$ dilepton events. To identify extra radiation, we used the PYCELL subroutine with a cone size of $R = 0.4$. Any reconstructed jets were required to be $\Delta R > 0.4$ away from the b partons to be considered “extra radiation”. As the matrix elements used by PYTHIA are LO, the lepton and antilepton distributions are the same, and the fully inclusive asymmetry is zero. The situation is more interesting when extra radiation is demanded or vetoed. In particular, correlations can be introduced by the angular structure of the all-orders QCD showering simulated in the Monte Carlo. For example, in PYTHIA the parameters MSTJ(50) and MSTP(67) control the structure of the final state (MSTJ(50)) and initial state (MSTP(67)) showers. With the default values (the “on” value) for these two parameters, PYTHIA adds initial- and final-state radiation to events based on color-flow information, while for the “off” value the showers develop independently of the color information and largely independently of the rest of the event. The color-flow constraint for the “on” case has the effect of restricting radiation to appear preferentially in the angular region between the p direction and the produced top quark direction, or between the \bar{p} direction and the anti-top quark direction. Thus the presence of extra radiation tends to be correlated with larger angle scattering of the top quark, *i.e.*, the top quark tends to be in the backward hemisphere when radiation is present. This correlation is intended to approximate the structure expected as a result of the “color coherence” in a full, all orders matrix element analysis with color singlet asymptotic states. Not only can this feature of PYTHIA lead to a non-zero lepton forward-backward asymmetry in the presence of extra radiation (even when integrated over the rapidity of the radiation), but this asymmetry has the same sign and general correlation with the radiation as in the earlier $t\bar{t}j$ perturbative analysis, as we now explore. Note that, by implication, the complementary event sample (with a veto on radiation) has an asymmetry of the opposite sign if the entire sample is to have a zero inclusive asymmetry. This means that the exclusive sample in PYTHIA will have an asymmetry of the same sign as the $t\bar{t}0j$ exclusive sample.

As in our earlier discussion of the matrix element calculations, CP invariance requires that the ℓ^- distribution is always mirror-antisymmetric to that of the ℓ^+ about $\eta(j) = 0$, $A_{FB}^{\ell^+}(\eta(j)) = -A_{FB}^{\ell^-}(-\eta(j))$. If the color-flow correlations in PYTHIA are turned “off” (MSTP(67) and MSTJ(50) “off”), the final state has no knowledge of the C (non-invariant) structure of the initial state and (as in the earlier discussion) $A_{FB}^{\ell^+}(\eta(j), \text{off}) = A_{FB}^{\ell^-}(\eta(j), \text{off})$ leading to a mirror-symmetric function of the jet rapidity $A_{FB}^{\ell}(\eta(j), \text{off}) = -A_{FB}^{\ell}(-\eta(j), \text{off})$. Thus the asymmetry need not vanish locally in $\eta(j)$, but must yield zero when integrated over a symmetric interval of the jet rapidity ($-\eta_0 > \eta(j) > \eta_0$). The p_T correlation of Eq. 7 is such an integrated quantity and is exhibited in Fig. 8. This figure provides a comparison of $A_{FB}^{\ell^+}$ between the PYTHIA results with the color-flow correlation “off” (MSTP(67) and MSTJ(50) “off”, the solid curve), PYTHIA results with the color-flow correlation “on” (the dashed curve) and the results of the NLO matrix element calculation (the dot-dashed curve), which we already considered in Fig. 2. As expected, the “off” curve is consistent with zero, while the “on” PYTHIA result and the NLO matrix element calculation exhibit comparable, negative values for $A_{FB}^{\ell^+}$ ($A_{FB}^{\ell^-}$ has

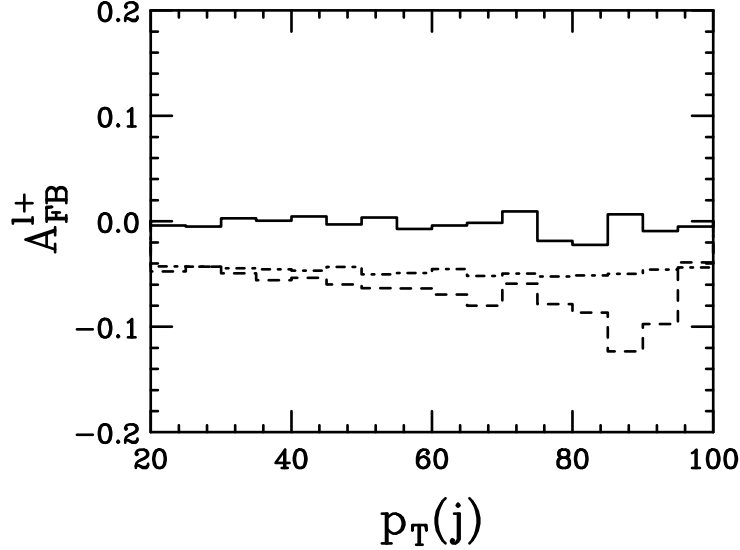


FIG. 8: Asymmetry $A_{FB}^{\ell^+}$ as a function of extra jet p_T with PYTHIA color-flow correlations turned off (solid) and on (dashed), as compared with the matrix element prediction (dot-dashed).

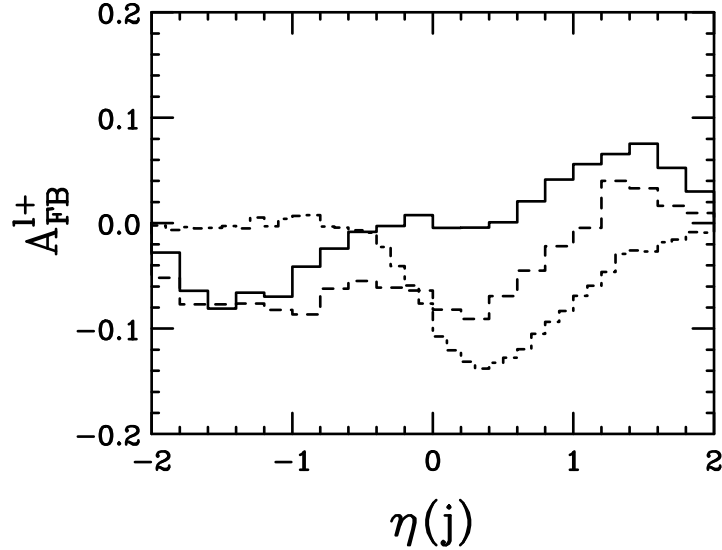


FIG. 9: Asymmetry $A_{FB}^{\ell^+}$ as a function of extra jet pseudorapidity $\eta(j)$ with PYTHIA color-flow correlations turned “off” (solid) and “on” (dashed), as compared with the matrix element prediction (dot-dashed).

equal magnitude but the opposite sign) with little p_T dependence.

Similarly to our earlier discussion, the variation of the asymmetry as a function of the jet rapidity is a richer subject as displayed in Fig. 9. As already argued the PYTHIA “off” results show a mirror-antisymmetric function of the jet rapidity, $A_{FB}^{\ell}(\eta(j), \text{off}) = -A_{FB}^{\ell}(-\eta(j), \text{off})$, which integrates to zero over a symmetric $\eta(j)$ interval. In this case the “no radiation” exclusive sample will exhibit no asymmetry. Note that the “off” distribution in Fig. 9 is similar in shape to the gg subprocess results in Figs. 3 and 5, but with the opposite sign. The sign of the asymmetry correlation can be understood by noting that in the color-flow correlation “off” PYTHIA calculation the asymmetry arises predominantly

from cases where the extra jet comes from final state radiation (FSR) with the jet and the $t\bar{t}$ pair in the same hemisphere. This is to be contrasted with the gg subprocess NLO matrix element calculation where the extra jet is recoiling from the $t\bar{t}$ pair and tends to be in the opposite hemisphere. As indicated in Fig. 9 for the color-flow correlation “on” case (and the real matrix element result) the asymmetry knows about the C non-invariant structure of the initial state allowing a variety of features: $A_{FB}^{\ell^+}(\eta(j), \text{on}) \neq A_{FB}^{\ell^-}(\eta(j), \text{on})$, $A_{FB}^{\ell}(\eta(j), \text{on}) \neq -A_{FB}^{\ell}(-\eta(j), \text{on})$, and $A_{FB}^{\ell}(\eta(j), \text{on})$ yields a non-zero net value when integrated over the jet rapidity. The fact that the net asymmetry for ℓ^+ is negative (positive for ℓ^-) arises not from these symmetry considerations, but rather the details of the correlations. The corresponding “no radiation” complement has an asymmetry of the opposite, *i.e.*, positive, sign (for ℓ^+).

We can analyze the PYTHIA calculations in somewhat more detail by separately turning “on” and “off” color-flow correlations, initial state radiation (ISR, as defined in PYTHIA) and final state radiation (FSR, as defined in PYTHIA). (Note that, due to interference effects there is no directly analogous analysis possible for the matrix element calculation.) The corresponding curves are exhibited in Fig. 10 for both ℓ^+ (solid) and ℓ^- (dashed). (The case with all parameters set to “on” is the dashed curve in Fig. 9 and the case with all radiation “on” but color-flow correlations “off” is the solid curve in Fig. 9.) As suggested earlier, we see in Fig. 10 a) and c) that with no color-flow correlations $A_{FB}^{\ell^+}(\eta(j), \text{off}) = A_{FB}^{\ell^-}(\eta(j), \text{off})$. On the other hand in Fig. 10 b) and d) with color-flow correlations present we have $A_{FB}^{\ell^+}(\eta(j), \text{on}) \neq A_{FB}^{\ell^-}(\eta(j), \text{on})$. From Fig. 10 a) we learn that ISR without color-flow correlations yields just a small (mirror-antisymmetric) asymmetry with the radiation in the opposite direction from the $t\bar{t}$ pair, while the addition of color-flow correlations in b) yields a much larger asymmetry with the t quark recoiling from (moving opposite to) the radiation (with the \bar{t} approximately at rest) for forward radiation and the \bar{t} moving forward (with the t approximately at rest) for backward radiation. It is this structure that is qualitatively similar to the $q\bar{q}$ subprocess matrix element result that dominates in Fig. 3. Comparing Fig. 10 c) and d) we see that the FSR contribution corresponds to the $t\bar{t}$ pair and the radiation all tending to move in the same direction, and that this mirror-antisymmetric structure is only slightly modified when color-flow correlations are present. Further, it is the FSR contribution that defines the qualitative shape of the combined result with no color-flow correlations present (the solid curve in Fig. 9). The combined result including color-flow correlations, the dashed curve in Fig. 9, has a shape that interpolates between Fig. 10 c) and Fig. 10 d). However, since the FSR contribution in d) is close to mirror-antisymmetric, it is the ISR contribution in b) that dominates any symmetric integral over this distribution.

The lesson here is that, even though PYTHIA does not (cannot) exhibit the inclusive forward-backward asymmetry characteristic of NLO QCD, PYTHIA does include parameters that can be set to produce events with much of the correlated asymmetry structure of NLO QCD. However, the agreement is only qualitative. *In detail* the asymmetries in the PYTHIA event samples have neither the same magnitude nor the same dependence on the extra radiation as the matrix element prediction, *i.e.*, the dashed and dot-dashed curves in Figs. 8 and 9 are distinct. At least one underlying difference is that PYTHIA includes FSR from the b quark in the top decay, which we do not include in the matrix element calculations. To the extent that the color-flow structure in PYTHIA correctly reflects coherence effects in the higher order showering corrections, beyond NLO, the asymmetries exhibited by PYTHIA are suggestive of what higher-order perturbative analyses will yield.

We have not studied HERWIG [15] extensively except to confirm that the inclusive asym-

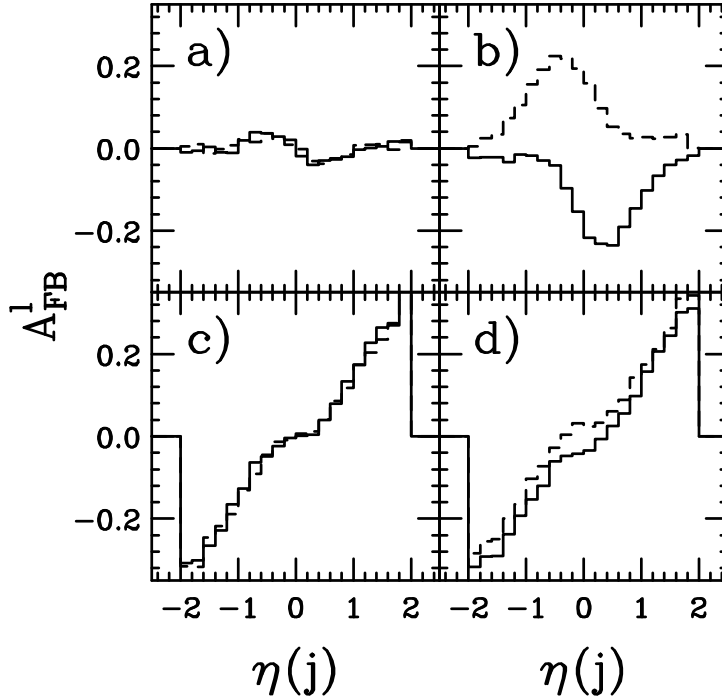


FIG. 10: Asymmetry A_{FB}^{ℓ} as a function of extra jet pseudorapidity $\eta(j)$ for ℓ^+ (solid) and ℓ^- (dashed) for the following choices of PYTHIA parameters: a) with color-flow correlations turned “off”, ISR “on” and FSR “off”; b) with color-flow correlations turned “on”, ISR “on” and FSR “off”; c) with color-flow correlations turned “off”, ISR “off” and FSR “on”; d) with color-flow correlations turned “on”, ISR “off” and FSR “on”.

metry is not present. It may or may not have correlated asymmetries similar to those observed with PYTHIA arising from color-flow related constraints on extra radiation from showers. We have performed no analogous analyses with SHERPA [16]. However, future studies using these generators should be aware that these correlated asymmetries may be present. In any case, it is clear that the experimental study of asymmetries, both inclusive and exclusive, can yield information about the coherence structure of QCD showers. To the extent that top quark physics is a background in studies of physics beyond the Standard Model, we must come to understand quantitatively these correlations and asymmetries in Monte Carlo simulations.

VII. CONCLUSIONS

Top quark pair production at a $p\bar{p}$ collider exhibits a forward-backward asymmetry due to higher-order short-distance QCD effects. This has been known for almost two decades, but only at an abstract theoretical level. Contributions to the asymmetry arise both from virtual corrections to $q\bar{q} \rightarrow t\bar{t}$, due to interference between the color-singlet box (4-pt.) and Born terms, and from real gluon emission in the same subprocess, due to interference of emission between the initial and final states (although one cannot think of it physically so simply, because those and other diagrams for emission are gauge-related). The two contributions are opposite in sign and of similar magnitude, leading to a partial cancellation which leaves a smaller asymmetry in the inclusive sample of the same sign as the virtual piece.

We have explored the asymmetry here with an eye toward experimental measurement. There are several major new points. First, experimentally the most reliable avenue for measuring the asymmetry is likely via the charged leptons, where both the direction and the sign of the charge can be determined with confidence. Unfortunately, we cannot test this approach in detail for an inclusive $t\bar{t}$ sample without a (currently unavailable) full NLO calculation including the t decays. For the $t\bar{t}j$ sample (requiring extra radiation), where the asymmetry appears at lowest non-trivial order, our results do confirm that the asymmetry at the top quark level is reflected in the top quark decay products, although with different magnitude. This change in the magnitude is due to the top quarks' spins leading to decay products being emitted preferentially in certain directions, which can move them from one hemisphere to another. Secondly, we have pointed out that the asymmetry of the leptons in the $t\bar{t}j$ sample is correlated with the angular distribution of additional jets in the event, but not their transverse momentum. Unfortunately, the real-emission asymmetries, which we term the $t\bar{t}j$ and $t\bar{t}jj$ components, are presently known only at LO. These last aspects of the short-distance asymmetry were not previously noticed in the literature. Finally we have studied the likely numbers of events at the Tevatron for the fully inclusive $t\bar{t}$ sample, where we assume the leptonic asymmetry is equal to the top-quark asymmetry, the radiation-required $t\bar{t}j$ sample, and the jet-veto-based exclusive $t\bar{t}0j$ sample. In all cases statistics will be an issue at the Tevatron, requiring a multiple channel analysis with (hopefully) outstanding accelerator and detector performance.

We have also shown that some models for color-flow correlations in QCD showers can yield correlated asymmetries as well, as exemplified in the parton shower Monte Carlo PYTHIA[14]. While the lepton asymmetry always vanishes in the totally inclusive PYTHIA-generated sample, when the relevant shower parameters are set (to the default values) to exhibit a specific model of color-flow structure in the parton showers, a negative top quark asymmetry arises in the $t\bar{t}j$ component with a positive asymmetry in the corresponding exclusive $0j$ component. Both the overall magnitude of the asymmetry and the differential asymmetry with respect to the additional hard jet angular distribution are qualitatively similar to but different in detail from those predicted by the perturbative NLO results.

We again emphasize that we have tried to explore only the general structure of the $t\bar{t}$ asymmetry signal and that, due to a number of limitations in the current theoretical tools, our results should not be regarded as precise predictions. We review here the major sources of those uncertainties/questions, which should be considered as areas that theorists need to address in the near future:

- How does the inclusive asymmetry change once kinematic cuts are imposed on the decay products? No NLO calculation exists to address this question.
- What is the overall $t\bar{t}j$ normalization, which is known presently only at LO? Additionally, we need to evaluate the NLO rate including decays so that cuts may be imposed.
- What is the effect of radiative top quark decays on experimental efficiencies for correctly selecting the extra jet in the inclusive production-radiation $t\bar{t}j$ sample? We need this to be able to isolate the maximally-asymmetric region in $\eta(j)$.
- We need to properly merge the $t\bar{t}j$ matrix elements into the parton-shower Monte Carlo environment in order to be able to make complete predictions.

While the experimental measurement of the asymmetries described here will likely be a challenge at the Tevatron due to limited statistics, it is still an extremely important goal. Since top quarks may well have a unique connection to new physics, and since they play a large role as a background in many new physics searches, Tevatron experimentalists should strive to determine top quark properties as accurately as possible. Further, the analysis of the correlation between the asymmetry and extra radiation may offer a nearly unique opportunity to elucidate detailed properties of long-distance, all-orders QCD, *i.e.*, the color-flow structure of the parton shower. While the measurement of A_{FB}^ℓ is unlikely to be a direct probe for new physics, unless the new physics contributions to the asymmetry are extremely large or of opposite sign to the SM, this measurement still provides a good example of the subtle behavior of SM particles in unexpected places. We should understand the SM as well as possible, from both theory and data, before moving on to see what lies beyond.

Acknowledgments

This research was supported in part by the U.S. Department of Energy under grant Nos. DE-FG02-91ER40685 and DE-FG02-96ER40956. D.R. would like to thank Regina Demina and Paul Tipton for advice on capabilities of the DØ and CDF detectors in Run II, while S.D.E. and M.T.B. thank Gordon Watts, Henry Lubatti, Toby Burnett and Matt Strassler for many helpful conversations.

-
- [1] F. Abe *et al.* [CDF Collaboration], Phys. Rev. D **50**, 2966 (1994);
S. Abachi *et al.* [D0 Collaboration], Phys. Rev. Lett. **74**, 2632 (1995).
- [2] A. Djouadi, arXiv:hep-ph/0503172, arXiv:hep-ph/0503173.
- [3] P. Azzi *et al.* [CDF and DØ Collaborations], arXiv:hep-ex/0404010.
- [4] V. M. Abazov *et al.* [D0 Collaboration], Nature **429**, 638 (2004).
- [5] D. Chakraborty, J. Konigsberg and D. L. Rainwater, Ann. Rev. Nucl. Part. Sci. **53**, 301 (2003) [arXiv:hep-ph/0303092].
- [6] See e.g. talk by C. Ciobanu at the Fermilab User's Meeting, June 8-9, 2005.
- [7] S. Vejcik, talk presented at Top Thinkshop 2, Fermilab, Nov. 11, 2000.
- [8] F. Halzen, P. Hoyer and C. S. Kim, Phys. Lett. B **195**, 74 (1987).
- [9] J. H. Kuhn and G. Rodrigo, Phys. Rev. Lett. **81**, 49 (1998);
J. H. Kuhn and G. Rodrigo, Phys. Rev. D **59**, 054017 (1999).
- [10] R. Brown, K. Mikaelian, V. Cung and E. Paschos, Phys. Lett. B **43**, 403 (1973);
F. A. Berends, K. J. F. Gaemers and R. Gastmans, Nucl. Phys. B **63**, 381 (1973);
S. J. Brodsky, C. E. Carlson and R. Suaya, Phys. Rev. D **14**, 2264 (1976);
F. A. Berends, R. Kleiss, S. Jadach and Z. Was, Acta Phys. Polon. B **14**, 413 (1983).
- [11] P. Nason, S. Dawson and R. K. Ellis, Nucl. Phys. B **303**, 607 (1988),
Nucl. Phys. B **327**, 49 (1989) [Erratum-ibid. B **335**, 260 (1990)];
W. Beenakker *et al.*, Nucl. Phys. B **351**, 507 (1991).
- [12] J. M. Campbell and R. K. Ellis, Phys. Rev. D **60**, 113006 (1999),
Phys. Rev. D **62**, 114012 (2000), Phys. Rev. D **65**, 113007 (2002).
- [13] J. Pumplin *et al.*, JHEP **0207**, 012 (2002).
- [14] H. U. Bengtsson and T. Sjostrand, Comput. Phys. Commun. **46**, 43 (1987);
T. Sjostrand, L. Lonnblad, S. Mrenna and P. Skands, arXiv:hep-ph/0308153.
- [15] G. Marchesini *et al.*, Comput. Phys. Commun. **67**, 465 (1992);
G. Corcella *et al.*, arXiv:hep-ph/0210213.
- [16] T. Gleisberg *et al.*, JHEP **0402**, 056 (2004).
- [17] A. Brandenburg, S. Dittmaier, P. Uwer and S. Weinzierl, in progress;
see also: Nucl. Phys. Proc. Suppl. **135**, 71 (2004).
- [18] D. Acosta *et al.* [CDF Collaboration], Phys. Rev. D **71**, 052003 (2005); T. Maruyama [CDF],
Eur. Phys. J. C **33**, S677 (2004).
- [19] T. Stelzer, F. Long, Comput. Phys. Commun. **81** (1994) 357.
- [20] B. W. Harris, E. Laenen, L. Phaf, Z. Sullivan and S. Weinzierl, Phys. Rev. D **66**, 054024
(2002); R. Bonciani, S. Catani, M. L. Mangano and P. Nason, Nucl. Phys. B **529**, 424 (1998);
M. Cacciari *et al.* JHEP **0404**, 068 (2004).
- [21] R. Demina, private communication.
- [22] P. Tipton, private communication.
- [23] L. Lyons, "Statistics For Nuclear And Particle Physicists," Cambridge University Press, Cambridge, 1986.
- [24] L. H. Orr, T. Stelzer and W. J. Stirling, Phys. Rev. D **52**, 124 (1995) [arXiv:hep-ph/9412294].